

Can “Electric Flare Stacks” Reduce CO₂ Emissions? A Case Study with Nonthermal Plasma

Matteo Molteni, Gary Walker, Dixit Parmar, Mike Sutton, Peter Licence, and Simon Woodward*



Cite This: <https://doi.org/10.1021/acs.iecr.3c02909>



Read Online

ACCESS |



Metrics & More

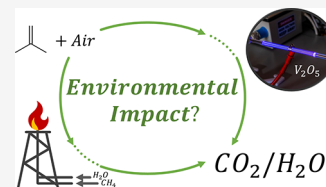


Article Recommendations



Supporting Information

ABSTRACT: Gas flare stacks are the current benchmark technology for industrial pollution control. However, their impact on human health and the environment is not negligible. If net zero CO₂ emissions are to be achieved, their current significant CO₂ impact (400 Mt y⁻¹ globally, 2022) should be reduced. Herein, a model nonthermal plasma “electric flare stack” consuming 6.6% less energy than an equivalent steam aided methane flare, with significant CO₂ emission reductions (between 2.0× and 11.4× lower), when removing isobutylene is demonstrated. Isobutylene streams in air (1.3% v/v) are completely and rapidly consumed (>99% at flow rates up to 125 mL min⁻¹, 1 atm, RT) by the electrically generated nonthermal plasma in a linear flow reactor. At low powers (≤50 J L⁻¹ specific input energy), the major degradation products (>95%) are a complex mixture of low-molecular-weight oxygenates, including acetone, isobutylene oxide, and isobutyraldehyde. Only small amounts of CO/CO₂ (<5% selectivity) are generated (at 50 J L⁻¹). Complete oxidation of isobutylene to CO₂ (>99% selectivity) results when the plasma oxidation is coupled to a heterogeneous catalyst bed. For the optimal V₂O₅ catalyst, synergistic interactions between the plasma and V₂O₅ are evident, as positioning the catalyst after the plasma provides optimal reactor performance (two-stage vs single-stage oxidation). Placement of shorter catalyst beds close to the plasma discharge region gives optimal reactor performance.



1. INTRODUCTION

Flare stacks are ubiquitous pollution control technologies in current industrial chemistry. Typically, methane is used to burn off gases and undesired products that otherwise would be released into the atmosphere. While this does remove pollutants, CO₂ emissions are increased. The World Bank estimates that 140 billion m³ of methane was flared in 2022, leading to the direct emission of 400 Mt of CO₂.¹ In addition, noncomplete combustion flare processes also lead to the release of some methane, whose greenhouse gas effect is estimated to be 27–30× higher than CO₂ over 100 years and 81–83× higher than CO₂ over 20 years.² Moreover, these incomplete combustion processes also produce a variety of hazardous gases, including acetylene, ethylene, benzene, styrene, and naphthalene,³ some of which have adverse effects on human health.

While the toxicity of flare stack emissions can be mitigated by building them in remote areas, CO₂ emission still results. Alternative technologies, replacing methane use with more sustainable alternatives, are needed. Without methane cocombustion, off-gas oxidation processes can be envisaged by using renewable energy-driven nonthermal plasmas (NTPs). In this paper, we study the destruction of a small carbon-based molecule (isobutylene) driven by electrical discharge and provide an energetic/CO₂ comparison of its destruction capability to an equivalent traditional methane-based flare stack.

The degradation of small carbon-based molecules with nonthermal plasma (NTP) has received increased attention in the past few years. NTP has been studied for the remediation

of volatile organic compounds (VOCs)^{4–8} and other atmospheric pollutants, such as SO_x or NO_x.^{9–11} Plasma destructive processes have clear potential to be a more sustainable VOC removal technique. Since NTPs are generated electrically, the start-up times are extremely rapid, and there is no need to wait for the system to reach a steady-state operation condition (as in a conventional flare stack). Plasma energy input can be easily and quickly adjusted to match the VOC remediation capability required. Potentially, this allows the development of efficient processes, where the discharge parameters are continuously optimized based on the destructive capability required, avoiding unnecessary energy waste. As plasma systems are modular, scale-up is simply achieved by increasing the number of plasma modules operating in parallel.

Reactive nonthermal plasmas are generated within an electrical discharge, whereby highly energetic electrons collide with ground-state gas molecules to produce a wide range of active species (excited species, ions, and radicals).^{12,13} These high-energy species can efficiently overcome activation barriers, promoting even challenging chemical reactions. While NTP is generated in the gas phase, if this is carried

Received: August 18, 2023

Revised: October 18, 2023

Accepted: October 19, 2023

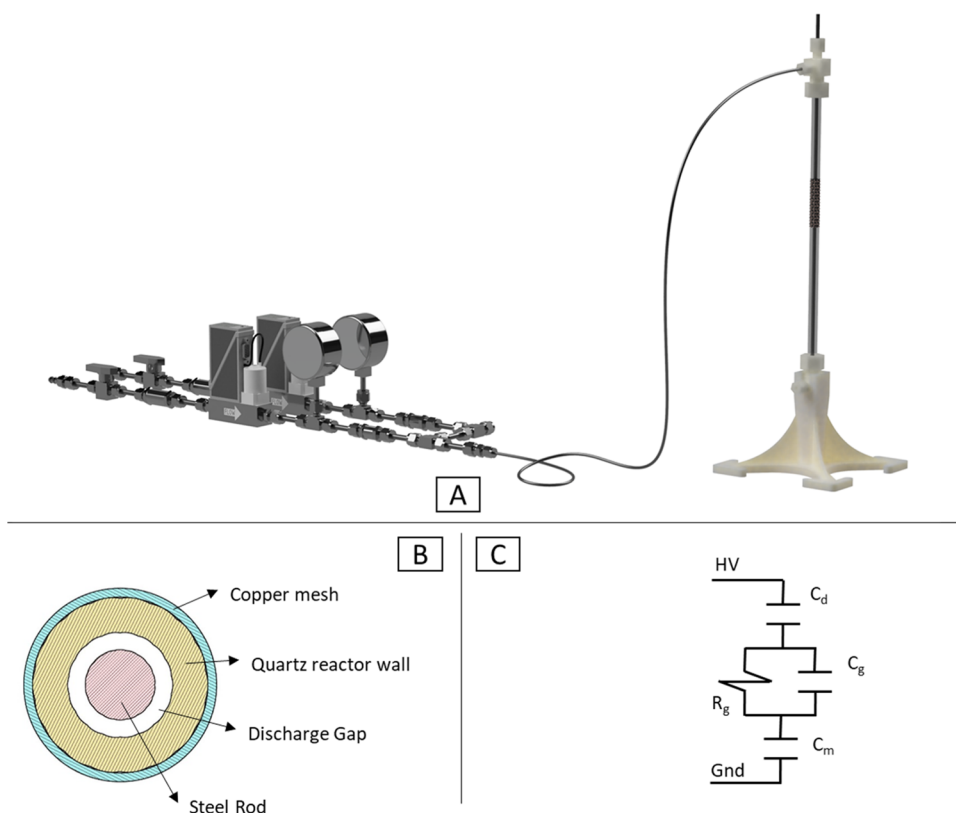


Figure 1. Schematic representation of the experimental apparatus. (A) Mass flow controller and the plasma reactor are shown. (B, C) Schematic representation of the dielectric barrier discharge configuration and the electrical equivalent circuit.

out in proximity to a catalyst, synergistic effects can be observed further reducing energy barriers and enhancing reactivities and selectivities.^{9,14} Two reaction configurations are commonly used: either the heterogeneous catalyst can be placed inside the NTP region (in plasma catalysis/1-stage configuration) or after the NTP (postplasma catalysis/2-stage configuration).

This paper reports the destructive capability of plasma to remediate waste streams containing isobutylene. Isobutylene is used at bulk scales (>8 Mt with a market size of 24.35 billion\$ in 2019) for use in a wide range of products, including car tires, adhesives, fuel additives (lubricants), coatings, and seals.¹⁵ Under room temperature and atmospheric pressure conditions, isobutylene is a gas. Its reactivity with photochemically generated ozone-based oxidants is relatively fast^{16,17} and its stratosphere half-life has been estimated to span 7.5–23 h.¹⁸ Data about the global warming potential of isobutylene are not readily available because of its short atmospheric persistence. However, it is known that decomposition of isobutylene leads to the formation of ethylene, propylene, butadiene, methane, and hydrogen, some of which have significant impacts.^{19,20} Methane and hydrogen exhibit, for instance, a global warming potential, respectively, 27–30 \times and 4.3 \times higher than CO₂. In addition, such isobutylene decomposition products are a source of secondary photochemical pollutants in their own right.

From an industrial safety perspective, isobutylene is highly flammable. As it is heavier than air, isobutylene tends to pool close to the ground, generating significant fire and explosion hazards. Multiple accidents have been reported caused by isobutylene explosions in refineries or chemical plants.^{21–23}

For this reason, industrial waste isobutylene streams are typically remediated by natural-gas-powered flare stacks.

We wondered if more efficient removal of isobutylene by NTP could be realized based on two early outline studies by Kudryashov et al.^{8,24} In that work, isobutylene (16.7% v/v) in pure oxygen at room temperature and atmospheric pressure was treated with NTP. An overall isobutylene conversion of only 6.8% was attained, with the major products being isobutylene oxide, isobutyraldehyde, acetone, and methanol. Notably, very significant energy input was required (4.7 J mL⁻¹ of treated isobutylene/O₂ mixture, 1 atm, RT) in that study.

Herein, we report isobutylene oxidation in the presence of air-based nonthermal plasma. The process is analyzed in terms of isobutylene destruction efficiency and product selectivity at different specific input energy (SIE) levels of the plasma used. The use of catalytic promoters is also investigated using both 1-stage and 2-stage configurations, including optimization of the reactor geometries to optimize any synergy between the NTP electrical discharge and the catalytic materials used.

2. MATERIALS AND METHODS

2.1. General Setup. A linear reactor apparatus was used (Figure 1A). The input gas lines were provided by suitable sources connected to two Bronkhorst EL-Flow Select mass flow controllers (MFCs), which allow precise control over the gas flow in the range 0–150 Ncc min⁻¹ (1 Ncc is 1 mL of gas at 20 °C (RT) and atmospheric pressure (1 atm)). An isobutylene cylinder (Air Liquid, impurities quoted as < 1 ppm) and a compressed air line (aerobic, O₂/N₂) acted as the active reagents for the reactor. The compressed air line was passed through a hydrocarbon and water removal filter prior to entering the reactor. After the MFCs, check valves were used

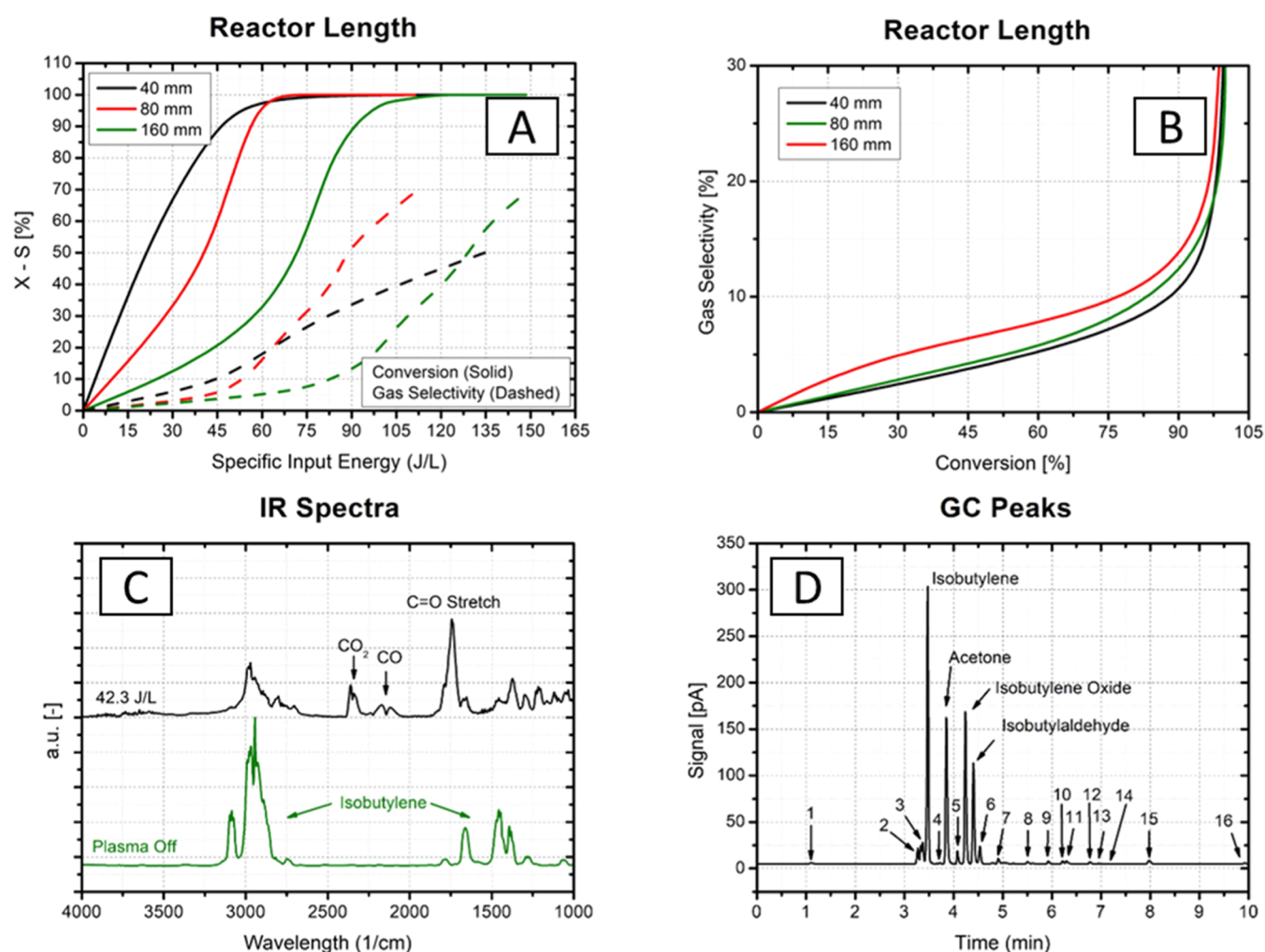


Figure 2. Plasma oxidation process in air. The results in terms of isobutylene conversion and carbon oxide selectivity (combined production of CO and CO₂) panel A with different copper mesh lengths (40, 80, and 160 mm) (A). The gas selectivity plotted as a function of the isobutylene conversion for the three cases considered (B). Infrared spectra (C) and the gas chromatography signal (D) are obtained with a low energy input.

to prevent back mixing and manometers are used to monitor reaction pressures. The gas mixture was fed to a quartz reactor tube (8 mm internal diameter × 300 mm length) through a PTFE hose to isolate the electronic devices from high voltages.

2.2. Plasma Generation. Nonthermal plasma was generated in a dielectric barrier discharge (DBD) reactor (Figure 1B) powered by a commercial power source (Leap100, Plasmaleap Technologies). The DBD reactor consisted of a quartz tube with an outer diameter of 10 mm and a wall thickness of 2 mm (Figure 1B); T-shaped connectors were used at each end of the reactor to allow for gas hose connections and for the placement of a steel rod (4 mm of diameter) along the tube axis. The plasma was generated in the small gap between the inner electrode (the steel rod) and the inner quartz wall of the reactor (Figure 1B). The extent of the plasma region was determined by the length of the outer electrode, a copper mesh wrapped around the quartz reactor tube. The DBD circuit configuration in Figure 1C was used. The quartz reactor wall can be represented as a capacitance (C_d), while the gas phase acts as a resistance (R_g) during a discharge and a capacitance (C_g) otherwise. An additional small capacitance is placed (C_m) between the inner electrode and the ground wire to allow for energy measurement.

Plasma was generated by applying a high voltage difference between the two electrodes (the inner steel rod and outer copper mesh). The presence of a dielectric material (the 2 mm thick quartz reactor) prevents the formation of arcs and limits the current flowing from one electrode to the other, keeping the power input low. The plasma power supply (Leap100) consists of two elements: a pulse generator and a transformer. The first generates short low-voltage pulses and allows us to modify the shape of the signal in terms of the voltage, frequency, and duty cycle. The voltage of the pulses then increased significantly with the use of a transformer.

Energy and power are measured with an oscilloscope (Tektronix MDO3014 2.5GS/s) with a high voltage probe (Tektronix P6015A 1000× attenuation). Another probe is also used to measure the voltage across the measuring capacitor ($C_m = 33$ nF),²⁵ which is then used to calculate the charge in the capacitor plates as a function of the total applied voltage (Lissajous plot). The energy measure is then obtained by the integration of the Lissajous plot. Additionally, a power monitor was placed in an electrical socket supplying the plasma unit itself. By doing so, both the specific energy delivered to the discharge and the total energy consumed by the power supply can be measured (see Appendix in the Supporting Information).

2.3. Catalysis and Product Analysis. In some runs, solid heterogeneous catalysts were used. Two different catalyst configurations were used: 1-stage (catalyst within the NTP zone) or 2-stage (catalyst after the NTP zone). Positional placement of the catalyst was done with the help of PTFE spacers fitting between the inner electrode and the inner wall of the glass reactor but allowing free gas flow. The spacers also allow for a more consistent placement of the inner electrode (always aligned along the axis of the reactor). A pad of quartz wool was placed after the catalytic bed to prevent particle loss. Finally, the reactor was kept in the vertical position with the gas flowing from the top to the bottom to limit any movement of the packed bed.

The analysis of the products was performed by using gas chromatography (GC) and infrared spectroscopy (IR) techniques. A gas chromatograph (Thermo Scientific Trace 1310) was equipped with an automatic sampling valve, a TraceGOLD TG-5MS column, and a flame ionization detector (FID). An infrared spectrometer (Bruker Alpha) detector was placed after the sampling valve of the GC to allow separate gas spectrum analysis.

3. RESULTS AND DISCUSSION

Initially, we investigated the degradation of isobutylene in the absence of any metal catalyst. These runs were conducted in the presence of a slight excess of aerobic oxygen (effective O₂/isobutylene molar ratio 6.8:1) so that the potential complete conversion to CO₂ is not oxidant limited. Fixing the flow rates at 124 mL min⁻¹ (air, 1 atm, RT) and 3.8 mL min⁻¹ (isobutylene, 1 atm, RT) allows the effects of the input energy and NTP reactor path length to be investigated (Figure 2).

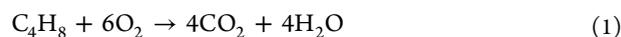
Figure 2A shows the isobutylene conversion (χ) and selectivity (S) toward CO₂ production as a function of the specific input energy (SIE) with different copper mesh lengths (40, 80, and 160 mm). The energy is varied by changing the duty cycle of the signal fed to the transformer while keeping the voltage and frequency constant. At a 40 mm mesh length, the isobutylene conversion increases rapidly with the SIE, and even at the lowest power setting available to us (21.97 J L⁻¹), 54.6% of the C₄H₈ feed is converted. Complete isobutylene conversion can be reached from 60 J L⁻¹ (green and black traces, Figure 2A) and further increasing the power affects only the CO₂ selectivity. The major gaseous product (see later for liquid products) detected is carbon dioxide, with some carbon monoxide also being formed. The selectivity to CO₂ increases more rapidly than that to carbon monoxide as a function of input power as expected for an ultimate product driven by thermodynamic factors.

The extension of the discharge volume is attained by extending the copper mesh used as the external electrode. By doing so, two different effects (Figure 2A) are achieved: (i) the residence time in the reactor increases and (ii) the same amount of energy is delivered to a wider volume, so the energy density decreases. By increasing the discharge volume, the gas spends more time in the reactor but with a lower energy density. The result is a lower conversion, as lower energy has been provided at an equivalent point in the reactor path. This suggests that the higher the energy density, the higher the concentration of active radical species formed within the plasma, which in turn boosts the conversion. As we do not use external cooling with our reactor, the operating temperature of the shorter configurations is significantly hotter (ca. 220 °C at 40 mm) than those of the longest (ca. 160 °C at 160 mm)

when using the same energy input. The selectivity toward carbon dioxide and monoxide is not affected by the SIE or the configuration. If the selectivity is plotted as a function of the conversion (Figure 2B), the curves overlap with each other, suggesting that plasma effects, not temperature, drive the gas selectivity in this reactor configuration.

However, CO₂ and CO are not the major products of these NTP-alone processes, and the combined CO_{*n*} (*n* = 1, 2) selectivity does not exceed 18%. Mainly medium to high boiling point oxygenates resulting from partial isobutylene oxidation are formed under these conditions. The less volatile oxygenates are detected as condensation products in off-gas reactor lines under all nonmetal-catalyzed plasma conditions. Such samples collected after representative runs are of similar composition to those detected (GC/IR) during midrun monitoring. Multiple peaks are observed in the IR signal and in the GC spectra (Figure 2C,D), resulting from the more volatile oxygenates. For example, in the IR spectrum (Figure 2C), the C–H alkene stretching of isobutylene (3000–3100 cm⁻¹) disappears even at low energy inputs, while a strong C=O stretch is detected. By comparing GC retention times (Figure 2D) against authentic samples, supported by GCMS, the major volatile liquid products are identified as acetone, isobutylene oxide, and isobutyraldehyde, although many minor oxidation products (1–16 Figure 2D) are present. Similar results have been obtained in the literature but require far higher energies.^{8,24} To further investigate oxygenate formation, we restricted the oxygen (air) available in runs of this type.

Isobutylene requires significant amounts of oxygen for its complete oxidation, 6 mol of O₂ per C₄H₈



By restricting the airflow to 10 mL min⁻¹ (1 atm, RT) at isobutylene flows of 3.8 mL min⁻¹ (1 atm, RT) a stoichiometry deficient in oxidant is attained (effective O₂/isobutylene molar ratio 0.55:1). Using a reactor length of 40 mm and an input energy of 1.69 J L⁻¹, the oxidation process struggles to reach complete isobutylene conversion (16.7%) and evidence of additional (partially oxygenated) species are apparent in the reactor IR spectra of the off-gas (Figure 3).

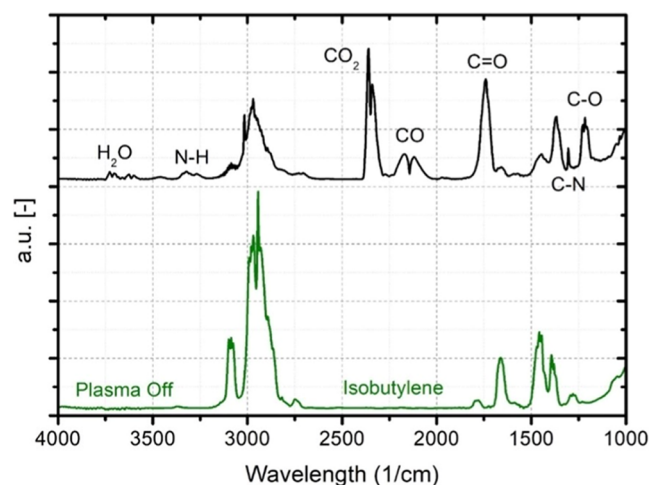


Figure 3. Infrared spectra of the plasma oxidation of isobutylene with oxygen as a limiting reagent. The spectrum measured with the discharge active is compared with the one obtained without, where only isobutylene is detected.

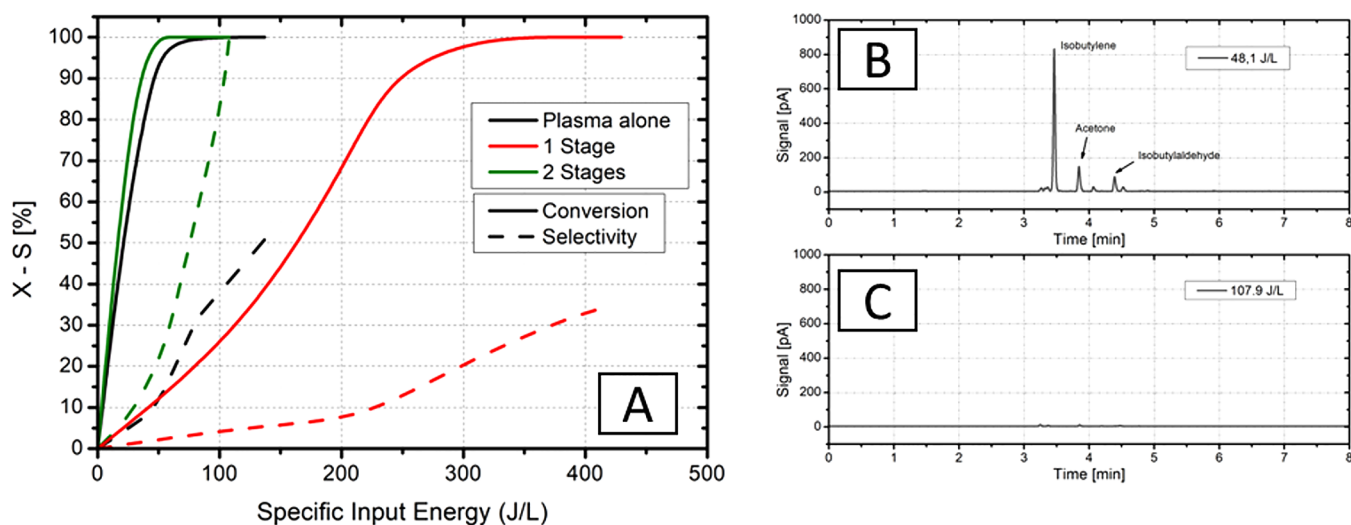


Figure 4. Synergistic effect between the plasma discharge and the catalysts. The isobutylene conversions of three configurations are compared in panel (A): (i) empty reactor (black line), (ii) 1-stage configuration (the catalyst inside the discharge, red line), and (iii) a 2-stage configuration (the catalyst after the discharge, green line), all using V_2O_5 . The GC spectra obtained for the 2-stage configuration are shown in panels B and C, respectively, for low and high input energy. At high input energy neither isobutylene nor combustion intermediates are detected (C).

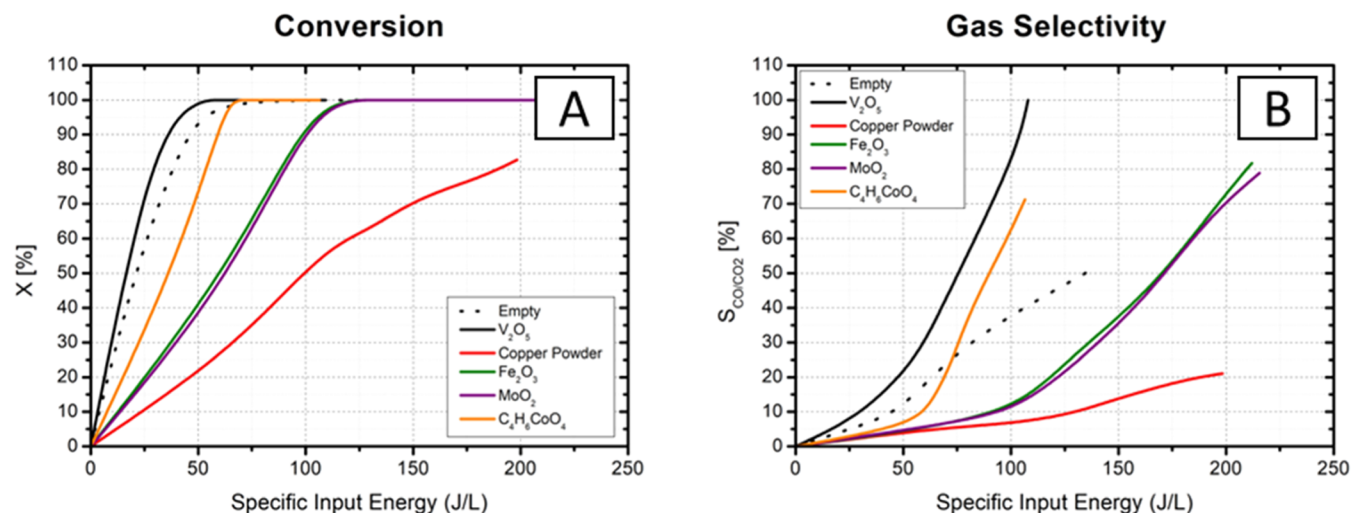


Figure 5. Results of the catalyst screening for the 2-stage configuration are presented in terms of isobutylene conversion (A) and carbon monoxide/dioxide selectivity (B). The catalysts used are vanadium oxide, copper powder, iron oxide, molybdenum oxide, and cobalt acetate.

The oxidation process clearly takes place even at low oxygen content, and CO and CO_2 are still observed as the gaseous products. Oxygen consumption is also apparent from the C=O and C–O stretching modes observed in the IR spectra of the volatile components. While Figure 2 is similar to Figure 1C, there are additional weaker bands that fall in the regions (ν_{N-H} , ν_{N-C}) expected for nitrogen bond formation. However, after such experimental runs, additional solid residuals can be isolated from inside the plasma reactor, which are of highly complex composition by NMR and MS analyses.

We sought to improve the selectivity of NTP isobutylene abatement to CO_2 by the introduction of a catalyst either directly inside or after the plasma discharge area. Using one of the small libraries of heterogeneous catalysts (V_2O_5 , Cu, Fe_2O_3 , MoO_3 , and $Co(acac)_2$), we first investigated the effect of the positioning of the catalyst in the quartz reactor tube using a fixed length of plasma discharge (40 mm) and V_2O_5 as a representative metal catalyst. The 1-stage combined NTP-metal-catalysis (V_2O_5 and NTP coaligned) performed worse

than that placing the V_2O_5 catalyst after the NTP zone (2-stage catalysis). In these studies, a 20 mm long catalyst bed placed 10 mm after the plasma was used for consistency. These results are summarized in Figure 4A, where the two configurations are also compared to the empty reactor. Upon increasing the input energy, more isobutylene is oxidized. At low energy input, isobutylene oxidation is not complete, and the main products are medium–high-boiling-point oxygenated compounds, as previously observed. At higher SIE, these intermediates are consumed, and carbon dioxide and carbon monoxide became the only products observed. The change in selectivity introduced by the catalyst is also depicted in panels B and C of Figure 4, where two spectra obtained at different energy input levels are shown. The data refers to the 2-stage configuration. At low SIE, the conversion (Figure 4B) is not complete, and multiple peaks are detected, indicating the presence of oxidation intermediates. Upon increasing energy input (Figure 4C), organic compounds and intermediates are no longer detected. The one-stage performance is shown in the

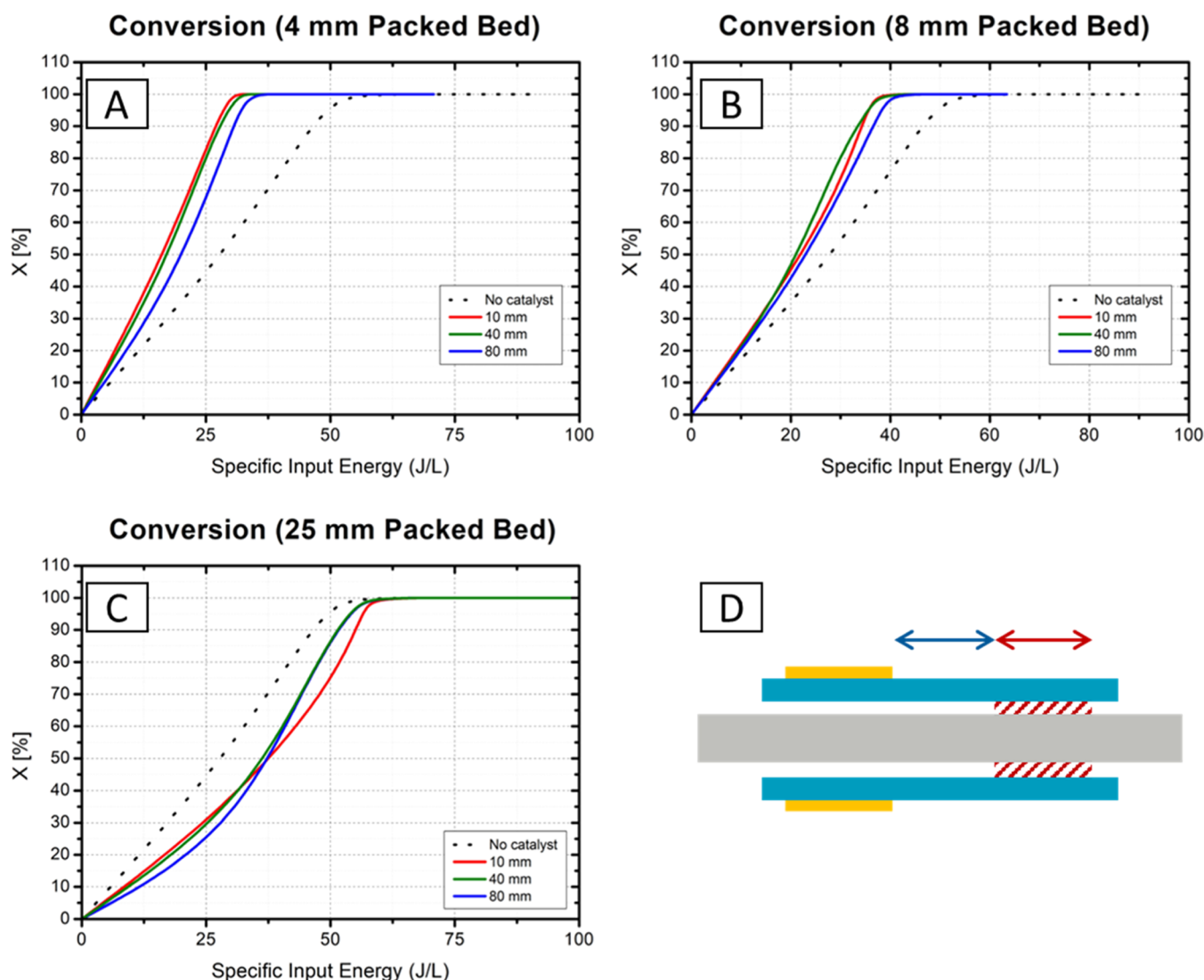


Figure 6. Geometrical optimization. The isobutylene conversions (A–C) are presented as a function of the specific input energy at different packed bed distances from the discharge area (10, 40, and 80 mm). In panels (A–C), the results obtained with an increasing packed bed length (4, 8, and 25 mm) are presented, respectively. The configuration used and the geometrical parameters changed are illustrated at the bottom (D).

red curves of Figure 4A. Full conversion is reached at 400 J L^{-1} , with a selectivity to gaseous products of 34%. With a 1-stage metal-NTP-oxidation configuration, significantly higher energy is required for equivalent conversion (almost $4\times$). The introduction of a catalytic material inside the discharge area is clearly detrimental. This behavior is likely due to two factors: (i) reduced efficiency of electrical discharge (plasma generation) and (ii) reduced reactor volume and consequently isobutylene residence time in the NTP zone.

The positioning of the catalyst (1-stage vs 2-stage) clearly plays a critical role in reactor product selectivity. Complete oxidation of isobutylene is attained at 100 J L^{-1} to $>98\%$ CO_2 (green dashed line, Figure 4A) in the 2-stage approach. For comparison, the selectivity to CO_2 does not exceed 30% in the reactor using NTP alone with the same energy input (black dashed line, Figure 4A). Control runs indicate that in the absence of discharge but with V_2O_5 , no conversion is obtained. The improvement in conversion and selectivity can be explained by the rising of synergistic effects between the plasma and the catalyst. The plasma initiates the combustion process, generating combustion intermediates, radicals, and

excited species that show higher reactivity on the catalyst surface.

Using a 2-stage configuration, screening of the other members of our catalyst library was carried out next. These results are presented in Figure 5, with comparison to the empty reactor performance as a reference (dotted curves). All of the catalysts present similar behaviors, but vanadium oxide clearly exhibits optimal performance in terms of both conversion and CO_2 selectivity. As discussed in a previous section, it reduces the energy required for complete conversion and it shifts the selectivity toward carbon dioxide and traces of carbon monoxide. For all the other catalytic materials trialed, a performance drop is observed compared to NTP alone. The worst results are obtained with copper powder, which required 200 J L^{-1} to reach a maximum conversion of 83%. At the same energy input, 100% conversion is obtainable with all other catalysts. The use of copper powder also leads to poor selectivity. Iron oxide and molybdenum oxide show a similar modest behavior, such that the curves almost completely overlap with each other. Cobalt acetate shows input energy-

dependent performance, worse than the plasma alone in the low-energy region, but it is better at high energy.

A set of experiments were performed to investigate the effects of reactor geometrical parameters on the NTP-V₂O₅-based process. Two easily optimized parameters for 2-stage oxidation are the distance between the discharge area and the catalyst and the length of the catalytic packed bed. We varied the first parameter from 10 to 80 mm and the second one from 4 to 25 mm. In all runs, we used vanadium (V) oxide, as it exhibits the best performance compared with the other materials tested in a previous section. The results are summarized in Figure 6, where the dotted curves in all graphs report the results of the empty reactor configuration. In the different panels (A–C), the results obtained by changing the packed bed length are presented, while in each panel, the effect of the distance from the discharge area of a specific packed bed length is shown. In Figure 6A, all of the curves obtained with this 2-stage configuration show better conversion compared to the empty reactor. The three curves obtained with the different distances (10, 40, and 80 mm) lie close to each other, but while the 10 and 40 mm curves almost overlap, the 80 mm curve is slightly shifted to the higher SIE value area. A similar behavior is also observed in the configuration with 8 mm (Figure 6B) packed bed length. The closer the catalyst is to the discharge area, the better the results are in terms of conversion. A shorter distance between the plasma and the catalyst allows more energetic plasma-derived species to reach the catalytic surface and react, facilitating catalysis. If the plasma–metal catalyst gap is too high, then the short-lived species do not have the lifespan to reach the catalyst region and the synergistic effects are not possible. Looking at the curves presented in Figure 6 in comparison with the results of the empty reactor, a negative effect can be noted upon increasing the packed bed length. Thus, in Figure 6A, 100% conversion is reached below 35 J L⁻¹ for all three curves, while in Figure 6B, the same conversion is reached only above 35 J L⁻¹. Moreover, when the catalyst bed length is further increased (Figure 6C, 25 mm), the overall reactor performance is worse than the empty reactor. This worsening of the conversion is likely due to the increased pressure in the discharge area due to the increasing size of the back pressure generated in the catalytic section. The resulting gas pressure increase affects the plasma properties (electron temperature and density) impacting the reaction rates. In this case, a pressure increase leads to a decrease of the electron temperature,²⁶ reducing the reaction rates in the plasma discharge. To compensate for the negative effect of the pressure, more energy needs to be provided, and the conversion curves shift to the right.

Finally, our optimal NTP isobutylene reactor was compared to traditional waste abatement technologies from both energetic and environmental standpoints. In this analysis, a gas flare is considered the standard reference technique for the remediation of waste products in industrial chemistry. A gas stream fed into a flare needs to satisfy a minimum requirement in terms of the flow heat energy content to allow an optimal combustion efficiency. This threshold is set to approximately 300 BTU scf⁻¹ by the NSPS (New Source Performance Standards) and the NESHAP (National Emissions Standards for Hazardous Air Pollutants), and it is calculated as the sum of the products between the enthalpy of combustions and the molar fractions of all of the combustible gases in a mixture (a comprehensive calculation is provided in the Appendix of the Supporting Information). We use this non-SI unit due to its

industrial prevalence, but note here that 300 BTU scf⁻¹ corresponds to about 11.8 J mL⁻¹ (1 atm, RT). If the waste stream heat (enthalpy) content is not high enough to reach the threshold, then natural gas (CH₄) is added to satisfy the above limit. The heat content of the gas mixture used in the plasma experiments (2.97% isobutylene in air) is only 88.03 BTU scf⁻¹, and methane would need to be added if a gas flare was used instead of the plasma discharge described herein. The power of a hypothetical “laboratory scale” gas flare stack (equivalent to our NTP rig) can then be estimated as the product of the combustion enthalpy and the flow of methane required to satisfy the threshold, which results in 11.8 J mL⁻¹ of gas treated. For a fair comparison between the two processes, this last value can be analyzed together with the total power used by the plasma power supply, which is 11.0 J mL⁻¹ (2-stage plasma catalysis with V₂O₅—100% conversion) per milliliter of gas treated. The plasma catalytic system shows ca. 6.6% lower power consumption than its methane gas flare equivalent. The difference becomes even larger when considering steam-assisted gas flares (as is commonly the case to avoid smoke production). The addition of water lowers the energy content of the gas stream, and additional methane is thus required for complete combustion.

NTP catalyst remediation also offers potential environmental impact improvement. For gas flare operations, a significant amount of methane gas is needed to guarantee complete remediation. Most of the carbon added is then emitted in the form of carbon dioxide. Conversely, only oxygen (or air) is needed for the nonthermal plasma process. For the same amount of isobutylene remediated, the equivalent methane flare generates ca. between 2.0× and 11.4× more CO₂ than the plasma-based “electric flare stack”. The impact of the gas flare is potentially even larger if its combustion is incomplete, as methane is released in the atmosphere (global warming potential approximately 25 times higher than CO₂). Presently, it is estimated that for every 33 tonnes of CO₂ emitted, 1 tonne of CH₄ is released directly in the atmosphere²⁷ in typical industrial applications (which is equivalent to 25 additional tonnes of CO₂, i.e., a 75% increase in emission burden). For full details of the comparison of the two processes, see the Appendix within the Supporting Information.

4. CONCLUSIONS

Oxidative isobutylene (C₄H₈) oxidation is possible by nonthermal plasma (NTP) discharge. High conversions of C₄H₈ are observed, even at low energy input. Complete thermodynamic oxidation to CO₂ is not realized with NTP alone even in the presence of excess O₂. Even after complete isobutylene conversion, further increasing the energy input does not improve the selectivity toward CO₂. The mass balance of the isobutylene is converted into a wider range of small oxygenated molecules, of which isobutylene oxide is major. The introduction of a metallic cocatalyst into the reactor is beneficial, but multiple aspects need to be optimized. Each catalyst shows a different interaction with the gas-phase molecules generated in the discharge. Vanadium (V) oxide has optimal performance in terms of conversion and selectivity. This cocatalyst not only reduces the energy input required to obtain 100% C₄H₈ conversion but also significantly improves the selectivity to CO₂. At low energy input (<72 J L⁻¹), oxygenates of isobutylene are still observed, but at increased input energy, near complete selectivity goes to carbon dioxide,

carbon monoxide, and water. The positioning of the V_2O_5 catalyst in relation to the discharge significantly affects the outcome. Placing the catalytic packed bed inside the discharge area has a detrimental effect on the oxidation process, leading to a significant increase in the energy requirements. However, a 2-stage configuration with V_2O_5 placed after the NTP zone improves the performance. The distance between the packed bed and discharge affects the interaction between the two processes. Finally, the pressure drop introduced by the cocatalytic material affects the discharge properties negatively, decreasing the plasma reaction rates.

Synergy of these positive and negative between the NTP and cocatalyst leads to an overall improvement (with V_2O_5) or a deterioration of the performance (all other catalysts screened). Further process improvements can be achieved by mitigating the negative effects. The reactor pressure drop, for instance, can be reduced by changing how the catalyst is introduced into the reactor. Replacing the packed bed with a thin layer deposition on a monolithic structure or directly on the inner surfaces of the reactor can reduce the pressure drop and improve the process.

A comparison between the plasma-enhanced waste abatement and an equivalent gas flare shows that there is a potential power reduction for the electrically driven process. Scaling-up of the NTP process is likely to further improve the energy efficiency of the plasma remediation system. Moreover, nonthermal plasma shows a significant reduction of the environmental impact of the remediation process, reducing by a factor between 2 and 11.4 (See [Supporting Information Appendix](#) for calculation details), the carbon dioxide emission over an equivalent size methane-based flare system. Thus, the answer to the question posed at the start of this paper appears to be “yes”, and we are pursuing further development of this technology.

■ ASSOCIATED CONTENT

SI Supporting Information

The Supporting Information is available free of charge at <https://pubs.acs.org/doi/10.1021/acs.iecr.3c02909>.

In-depth environmental analysis including all equations and assumptions used; energy measurement methodology adopted for the nonthermal plasma; conversion factors ([PDF](#))

■ AUTHOR INFORMATION

Corresponding Author

Simon Woodward – GSK Carbon Neutral Laboratories for Sustainable Chemistry, University of Nottingham, Nottingham NG7 2TU, U.K.; orcid.org/0000-0001-8539-6232; Email: simon.woodward@nottingham.ac.uk

Authors

Matteo Molteni – GSK Carbon Neutral Laboratories for Sustainable Chemistry, University of Nottingham, Nottingham NG7 2TU, U.K.; orcid.org/0000-0001-6603-8472

Gary Walker – Lubrizol Ltd., Derby DE56 4AN, U.K.

Dixit Parmar – Lubrizol Ltd., Derby DE56 4AN, U.K.;

orcid.org/0000-0002-6594-5932

Mike Sutton – Lubrizol Ltd., Derby DE56 4AN, U.K.

Peter Licence – GSK Carbon Neutral Laboratories for Sustainable Chemistry, University of Nottingham,

Nottingham NG7 2TU, U.K.; orcid.org/0000-0003-2992-0153

Complete contact information is available at: <https://pubs.acs.org/10.1021/acs.iecr.3c02909>

Notes

The authors declare no competing financial interest.

■ ACKNOWLEDGMENTS

The authors thank the University of Nottingham and the Lubrizol Prosperity Partnership (EPSRC: EP/V037943/1) for facilitating this research.

■ REFERENCES

- (1) Bamji, Z. 2022 *Global Gas Flaring Tracker Report* World Bank Publications: Washington, USA; 2022. <https://thedocs.worldbank.org/en/doc/1692f2ba2bd6408db82db9eb3894a789-0400072022/original/2022-Global-Gas-Flaring-Tracker-Report.pdf>.
- (2) International Energy Agency. *Global Methane Tracker 2023* <https://www.iea.org/reports/global-methane-tracker-2023>.
- (3) Strosher, M. T. Characterization of Emissions from Diffusion Flare Systems. *J. Air Waste Manage. Assoc.* **2000**, *50* (10), 1723–1733.
- (4) Vandenbroucke, A. M.; Morent, R.; De Geyter, N.; Leys, C. Non-Thermal Plasmas for Non-Catalytic and Catalytic VOC Abatement. *J. Hazard Mater.* **2011**, *195*, 30–54.
- (5) Qu, M.; Cheng, Z.; Sun, Z.; Chen, D.; Yu, J.; Chen, J. Non-Thermal Plasma Coupled with Catalysis for VOCs Abatement: A Review. *Process Saf. Environ. Prot.* **2021**, *153*, 139–158.
- (6) Veerapandian, S. K.; Leys, C.; De Geyter, N.; Moren, R. Abatement of VOCs Using Packed Bed Non-Thermal Plasma Reactors: A Review. *Catalysts* **2017**, *7* (4), 113.
- (7) Thevenet, F.; Sivachandiran, L.; Guaitella, O.; Barakat, C.; Rousseau, A. Plasma–Catalyst Coupling for Volatile Organic Compound Removal and Indoor Air Treatment: A Review. *J. Phys. D: Appl. Phys.* **2014**, *47* (22), No. 224011.
- (8) Kudryashov, S. V.; Shchegoleva, G. S.; Sirotkina, E. E.; Ryabov, A. Y. Oxidation of Hydrocarbons in a Barrier Discharge Reactor. *High Energy Chem.* **2000**, *34* (2), 112–115.
- (9) Van Durme, J.; Dewulf, J.; Leys, C.; Van Langenhove, H. Combining Non-Thermal Plasma with Heterogeneous Catalysis in Waste Gas Treatment: A Review. *Appl. Catal., B* **2008**, *78* (3–4), 324–333.
- (10) Talebizadeh, P.; Babaie, M.; Brown, R.; Rahimzadeh, H.; Ristovski, Z.; Arai, M. The Role of Non-Thermal Plasma Technique in NO_x Treatment: A Review. *Renewable Sustainable Energy Rev.* **2014**, *40*, 886–901.
- (11) Ma, S.; Zhao, Y.; Yang, J.; Zhang, S.; Zhang, J.; Zheng, C. Research Progress of Pollutants Removal from Coal-Fired Flue Gas Using Non-Thermal Plasma. *Renewable Sustainable Energy Rev.* **2017**, *67*, 791–810.
- (12) Turner, M. Physics of Cold Plasma. In *Cold Plasma in Food and Agriculture: Fundamentals and Applications*; Academic Press, 2016; pp 17–51 DOI: [10.1016/B978-0-12-801365-6.00002-0](https://doi.org/10.1016/B978-0-12-801365-6.00002-0).
- (13) Whitehead, J. C. The Chemistry of Cold Plasma. In *Cold Plasma in Food and Agriculture: Fundamentals and Applications*; Academic Press, 2016; pp 53–81 DOI: [10.1016/B978-0-12-801365-6.00003-2](https://doi.org/10.1016/B978-0-12-801365-6.00003-2).
- (14) Whitehead, J. C. Plasma–Catalysis: The Known Knowns, the Known Unknowns and the Unknown Unknowns. *J. Phys. D: Appl. Phys.* **2016**, *49* (24), No. 243001.
- (15) Isobutene Market Size, Share | Global Industry Report, 2024. <https://www.grandviewresearch.com/industry-analysis/isobutene-market>. (accessed 2023–05–09).
- (16) Atkinson, R.; Carter, W. P. L. Kinetics and Mechanisms of the Gas-Phase Reactions of Ozone with Organic Compounds under Atmospheric Conditions. *Chem. Rev.* **1984**, *84* (5), 437–470.

(17) Atkinson, R. Kinetics and Mechanisms of the Gas-Phase Reactions of the Hydroxyl Radical with Organic Compounds under Atmospheric Conditions. *Chem. Rev.* **1986**, *86* (1), 69–201.

(18) National Center of Biotechnology Information. Isobutylene. <https://pubchem.ncbi.nlm.nih.gov/source/hsdb/613>. (accessed 2023–07–04).

(19) Hurd, C. D.; Spence, L. U. The Pyrolysis of Hydrocarbons: Isobutylene. *J. Am. Chem. Soc.* **1929**, *51* (12), 3561–3572.

(20) Borrell, P.; Cashmore, P. Photolysis of Isobutene at 185 Nm. *Trans. Faraday Soc.* **1969**, *65*, 1595–1602.

(21) Association For The Study of Failure. Explosion of an Air Heater of a Boiler at an Agricultural Chemical Manufacturing Plant. <https://www.shippai.org/fkd/en/cfen/CC1200096.html>. (accessed 2023–07–04).

(22) CBS. CSB Factual Update into April 2019 KMCO Fire and Explosion. <https://www.csb.gov/csb-factual-update-into-april-2019-kmco-fire-and-explosion/>. (accessed 2023–07–04).

(23) FOX 26 Houston staff. One Death in Crosby-area Chemical Facility Fire. <https://www.fox26houston.com/news/one-death-in-crosby-area-chemical-facility-fire>. (accessed 2023–08–08).

(24) Kudryashov, S. V.; Ryabov, A. Y.; Sirotkina, E. E.; Shchegoleva, G. S. Oxidation of Propylene and Isobutylene in a Reactor with Barrier Discharge. *Russ. J. Appl. Chem.* **2004**, *77* (11), 1904–1906.

(25) Wang, R.; Yang, Y.; Chen, S.; Jiang, H.; Martin, P. Power Calculation of Pulse Power-Driven DBD Plasma. *IEEE Trans. Plasma Sci.* **2021**, *49* (7), 2210–2216.

(26) Yan, S.; Kamal, H.; Amundson, J.; Hershkowitz, N. Use of Emissive Probes in High Pressure Plasma. *Rev. Sci. Instrum.* **1996**, *67* (12), 4130–4137.

(27) IEA. Flaring Emissions, IEA, Paris. License: CC BY 4.0 2022 <https://www.iea.org/energy-system/fossil-fuels/gas-flaring>. (accessed: 2023–07–04).